

The adsorption of CO on charged and neutral Au and Au₂: A comparison between wave-function based and density functional theory

Peter Schwerdtfeger,^{1,a)} Matthias Lein,¹ Robert P. Krawczyk,¹ and Christoph R. Jacob²

¹Center of Theoretical Chemistry and Physics, The New Zealand Institute for Advanced Study, Massey University (Auckland Campus), Private Bag 102904, North Shore MSC, Auckland, New Zealand

²Department of Theoretical Chemistry, Faculty of Sciences, Vrije Universiteit Amsterdam, De Boelelaan 1083, 1081 HV Amsterdam, The Netherlands

(Received 4 December 2007; accepted 19 December 2007; published online 25 March 2008)

Quantum theoretical calculations are presented for CO attached to charged and neutral Au and Au₂ with the aim to test the performance of currently applied density functional theory (DFT) by comparison with accurate wave-function based results. For this, we developed a compact sized correlation-consistent valence basis set which accompanies a small-core energy-consistent scalar relativistic pseudopotential for gold. The properties analyzed are geometries, dissociation energies, vibrational frequencies, ionization potentials, and electron affinities. The important role of the basis-set superposition error is addressed which can be substantial for the negatively charged systems. The dissociation energies decrease along the series Au⁺-CO, Au-CO, and Au⁻-CO and as well as along the series Au₂⁺-CO, Au₂-CO, and Au₂⁻-CO. As one expects, a negative charge on gold weakens the carbon oxygen bond considerably, with a consequent redshift in the CO stretching frequency when moving from the positively charged to the neutral and the negatively charged gold atom or dimer. We find that the different density functional approximations applied are not able to correctly describe the rather weak interaction between CO and gold, thus questioning the application of DFT to CO adsorption on larger gold clusters or surfaces. © 2008 American Institute of Physics. [DOI: 10.1063/1.2834693]

I. INTRODUCTION

Although bulk gold is known to be chemically rather inert, nanosized gold clusters are found to exhibit surprising reactivity.¹⁻⁶ Gold nanomaterials have, therefore, become a center of immense research activity in the past decade,^{1,7} not only on the experimental side with a wide range of applications,^{1,8-25} but also on the theoretical side ranging from cluster simulations to extended surface calculations including catalytic reactions.²⁶⁻³⁴ Gold clusters come in a variety of interesting and unusual structure types such as tubes,^{35,36} pyramids,³⁷⁻³⁹ octahedrons,^{40,41} rings,^{42,43} or wires,⁴⁴⁻⁵³ such as helical gold nanowires by Kondo and Takayanagi.⁵⁴

Considerable interest has been devoted to the interaction of small gold clusters with CO, NO, or O₂.^{9,18,55-67} For example, the process involving CO is important in environmental control of exhaust fumes from combustion as gold is not as easily poisoned as other catalysts.^{1,68} Other important processes involve hydrogenation of carbon dioxide⁶⁹ or the water-gas shift reaction.^{70,71} Concerning theoretical studies on adsorption of molecules on charged or neutral gold clusters or gold surfaces, the most widely used approximation is density functional theory (DFT). It is, however, well-known that dispersive type of interactions (van der Waals) are not well described by common density functionals, and physisorption properties on gold surfaces may, therefore, suffer

from these defects.⁷² As CO is only weakly bound to gold,⁹ it becomes desirable to benchmark density functional calculations against more accurate wave-function based (*ab initio*) methods. Here, one faces, however, four main difficulties. First of all, accurate electron correlation procedures such as coupled cluster techniques soon become very expensive in computer time with increasing cluster size of gold. Such a procedure is currently not computationally feasible for larger gold clusters. Second, when the system becomes metallic, single-reference procedures with limited configuration interaction space will eventually fail. Third, the basis-set superposition error is well-known to be by far more important in wave-function based methods compared to density functional theory. This together with correctly describing the electron-electron interaction in correlation procedures lead to very large basis-set expansions in wave-function based theories. Fourth, relativistic effects cannot be neglected anymore for gold, as this is now a well documented fact.^{26,29,73-75} In this paper, we investigate the interaction of carbon monoxide with positively charged, neutral, and negatively charged Au and Au₂ by both DFT and wave-function based coupled cluster methods in order to address these fundamental questions.

II. COMPUTATIONAL DETAILS

We investigated the ground state structures of linear AuCO⁺ (C_{∞v}, ¹Σ⁺), bent AuCO (C_s, ²A'), bent AuCO⁻ (C_s, ¹A'), the end-on structures of linear Au₂CO⁺ (C_{∞v}, ¹Σ⁺), linear Au₂CO (C_{∞v}, ²Σ⁺), and bent Au₂CO⁻ (C_s, ²A'), and the CO bridged structures of C_{2v} symmetry which present

^{a)}Author to whom correspondence should be addressed. Electronic mail: p.a.schwerdtfeger@massey.ac.nz.

TABLE I. Exponents and contraction coefficients for the gold Gaussian SB set used in DFT and wave-function based calculations.

<i>l</i>	DFT basis		MP2 basis	
	Exponent	Coefficient	Exponent	Coefficient
<i>s</i>	16.900 220 171	-0.512 735 100	16.764 326 059	-0.507 464 100
	14.627 841 463	0.807 566 600	14.460 937 786	0.812 254 810
	5.817 139 365	-0.860 420 200	5.886 979 319	-0.860 420 200
<i>s</i>	1.415 476 507	1.000 000 000	1.432 006 949	1.000 000 000
<i>s</i>	0.656 816 591	1.000 000 000	0.724 816 809	1.000 000 000
<i>s</i>	0.169 879 887	1.000 000 000	0.242 296 077	1.000 000 000
<i>s</i>	0.061 782 999	1.000 000 000	0.074 087 594	1.000 000 000
<i>s</i>	0.020 820 398	1.000 000 000	0.027 467 300	1.000 000 000
<i>p</i>	9.458 603 187	-0.521 359 238	9.611 106 905	-0.532 088 440
	6.705 233 267	1.160 632 814	6.761 899 768	1.197 984 365
	1.940 810 945	-1.005 179 000	1.907 003 117	-1.005 178 664
<i>p</i>	1.031 129 896	1.000 000 000	1.083 572 768	1.000 000 000
<i>p</i>	0.449 108 097	1.000 000 000	0.464 418 001	1.000 000 000
<i>p</i>	0.139 894 095	1.000 000 000	0.181 551 000	1.000 000 000
<i>p</i>	0.084 927 807	1.000 000 000	0.070 886 610	1.000 000 000
<i>d</i>	4.676 373 225	-0.153 229 090	4.979 833 280	-0.164 653 805
	2.504 011 574	0.309 046 191	2.441 626 893	0.324 216 076
	1.028 849 121	0.680 332 900	1.238 174 946	0.680 332 908
<i>d</i>	0.401 702 103	1.000 000 000	0.548 230 910	1.000 000 000
<i>d</i>	0.138 529 054	1.000 000 000	0.184 287 978	1.000 000 000
<i>f</i>	2.418 550 170	-0.797 642 897	1.835 776 812	-0.439 769 038
	1.448 079 284	-0.627 922 900	0.804 595 519	-0.627 922 900
	0.988 023 012	1.001 059 042	0.313 133 701	-0.226 041 592

local minima on the potential energy surface, Au_2CO^+ (2B_2), Au_2CO (1A_1), and Au_2CO^- (2A_1). For some of these molecules, there are low lying excited electronic states which we did not investigate. A variety of density functionals was used, the local spin density approximation (LSDA),⁷⁶ the generalized gradient approximation using the Becke–Perdew BP86 and Perdew–Wang PW91 functionals,^{77,78} and a hybrid Becke–Lee–Yang–Parr functional containing exact exchange (B3LYP).^{79,80} For the wave-function based methods, we used single-reference second-order many-body perturbation theory (MP2) as well as coupled cluster singles-doubles with perturbative triples, [CCSD(T)].⁸¹ The full active orbital space was used in all these correlation calculations. For carbon and oxygen, Dunning’s augmented correlation-consistent triple valence basis sets were used (aug-cc-pVTZ),⁸² as diffuse functions are needed to correctly describe the weak interaction between CO and gold. For gold, we used a small-core energy-consistent scalar relativistic pseudopotential of the Stuttgart type.⁸³ For the basis set of gold, we developed a medium-sized compact correlation-consistent valence basis set obtained from a numerical energy minimization procedure at the MP2 level of theory. For the DFT calculations, we produced a similar basis set optimized at the LSDA level of theory. The final contraction scheme is $(7s5p5d3f)/[5s3p3d1f]$ and the exponents and contraction coefficients are listed in Table I. This small but compact basis set is denoted as small basis set (SB) for the following. At the optimized minimum geometry, the Hessian was obtained and a frequency calculation was carried out.

For the masses, the isotopes 12-C, 16-O, and 197-Au were used. For the dissociation energies, we considered the basis-set superposition error (BSSE) estimated from the counterpoise correction according to Boys and Bernardi.⁸⁴ Some of the calculations showed extremely large BSSEs and we, therefore, decontracted the *f*-function set and added one *g* function for gold with exponent of 0.8 [medium basis (MB) set] which results in a $(7s5p5d3f1g)/[5s3p3d3f1g]$ set. For AuCO^q and for some of the DFT calculations for Au_2CO^q with $q=-1, 0, +1$, we were able to increase the basis set even more in order to further reduce the BSSE, i.e., we used a $(8s6p6d4f3g1h)/[7s5p5d4f3g1h]$ set together with augmented correlation-consistent quadruple valence basis sets for both carbon and oxygen (aug-cc-pVQZ) (Ref. 82) [denoted as large basis (LB) set]. Here, the additional added functions have the exponents of 0.01 for *s*, 0.03 for *p*, 0.06 for *d*, 4.2 for *f*, and 0.8 for *h*, and the original *g*-function exponent has been substituted by the exponents of 3.6, 1.2, and 0.4. For Au_2CO , this leads to 604 Gaussian functions contracted to 400 basis functions.

III. RESULTS AND DISCUSSION

The ionization potentials and electron affinities for the gold atom are shown in Table II. We note that the B3LYP functional gives reasonable results as compared to the experiment, although none of the functionals perform exceptionally well for all properties of the Au_2^q ($q=-1, 0, +1$) molecules considered (Table III). In comparison, the CCSD(T) calculations give excellent results as expected, but rather large basis sets are required to get close to the experimental values. Tables II and III show that the basis sets applied are sufficiently accurate to describe the Au–Au bond. Using our LB set, the CCSD(T) values are in excellent agreement with experiment. In fact, our best ionization potential of 9.206 eV and electron affinity of 2.257 eV are in very good agreement with the Fock-space coupled cluster results of 9.101 and 2.278 eV, respectively by Eliav *et al.*,⁸⁵ who used the Dirac-Coulomb Hamiltonian. The binding of two Au atoms to form Au_2 results in a fully occupied σ -bonding orbital and, therefore, the ionization potential is expected to increase from Au to Au_2 . This is not immediately evident from the experimental values (Table II). However, all wave-function based methods give an increase in the ionization potential in contrast to the DFT results. In a similar argument, using the lowest unoccupied σ -antibonding orbital, the electron affinity should decrease from Au to Au_2 which is confirmed by experiment (Table II). This is now correctly described by all methods. Au^q and Au_2^q with $q=-1, 0, +1$ have been studied by many groups in the past (see the reference list given in Pyykkö’s review²⁶) and, therefore, is not discussed in great detail here. The question in this work is if the density functionals applied are able to accurately describe the Au–CO bond, which is an important issue for calculations of CO adsorption on gold nanoclusters.

The optimized bond parameters of AuCO^q with $q=-1, 0, +1$ are collected in Table IV. Except for the positively charged species we obtain bent geometries. For neutral AuCO , this is in agreement with an early work by

TABLE II. Adiabatic ionization potentials and electron affinities of Au, Au₂, AuCO, and Au₂CO (in eV). Experimental values from Refs. 66 and 86–89. SB set is used if not otherwise stated. CCSD value is at the optimized CCSD(T) geometry.

Method	Au		AuCO		Au ₂		Au ₂ CO	
	IP	EA	IP	EA	IP	EA	IP	EA
LSDA	10.325	2.964	8.451	2.429	10.273	2.556	9.879	1.711
BP86	9.685	2.362	7.965	1.971	9.503	2.080	9.093	1.360
PW91	9.583	2.258	7.883	1.880	9.399	1.976	9.003	1.276
PW91 ^a	9.619	2.363	7.884	1.875	9.481	1.997	9.067	1.251
B3LYP	9.404	2.150	7.766	1.873	9.243	1.907	8.773	1.234
B3LYP ^a	9.441	2.232	7.762	1.873	9.326	1.904	8.839	1.194
MP2	9.031	1.853	7.426	1.566	9.358	1.533	9.072	0.369
MP2 ^b	9.304	2.075	7.546	1.733	9.740	1.642	9.366	0.437
MP2 ^a	9.425	2.275	7.624	1.849	9.903	1.764
CCSD	8.767	1.753	7.218	1.342	8.789	1.567	8.375	0.653
CCSD(T)	8.830	1.873	7.334	2.313	8.960	1.626	8.590	0.699
CCSD(T) ^b	9.097	2.061	7.438	1.662	9.246	1.759
CCSD(T) ^a	9.206	2.257	7.516	1.823	9.384	1.886
Expt.	9.226	2.309	9.20 ± 0.21	2.01 ± 0.01
					9.16 ± 0.10			

^aLB set.

^bMB set.

Schwerdtfeger and Bowmaker.⁵⁶ There is quite a discrepancy in these bond parameters when the DFT results are compared with the more accurate coupled cluster data. For example, for the negatively charged AuCO⁻, the variation for r_{AuC} is more than 0.4 Å between the different functionals. The deviation from the coupled cluster result is much smaller for r_{CO} as one expects, but the AuCO angles for AuCO and AuCO⁻ vary widely. The B3LYP functional yields the longest Au–C bond distance, whereas the LSDA functional gives the shortest distance due to the well-known fact that LSDA overbinds. Nevertheless, if we compare to our best coupled cluster results obtained from using the LB set, the B3LYP functional performs perhaps best compared to all other functionals but still with deviations of about 0.9 Å for the Au–C distance and 15° for the Au–C–O angle from the CCSD(T) result of AuCO⁻. This is due to the fact that CO in AuCO⁻ is extremely weakly bound, and even at the coupled cluster level, it is difficult to correctly describe this weak interaction as extending the basis set leads to a significant elongation of the Au–CO bond and to a very small Au–C–O bond angle. We mention that the bond distances of free CO using the LB set are 1.134 Å at the PW91, 1.124 Å at the B3LYP, and 1.133 Å at the CCSD(T) level of theory [expt. is 1.128 Å Ref. 90]. This implies that the CO bond becomes elongated upon binding to Au⁺, Au and Au⁻. The situation somewhat improves for AuCO⁺. However, for neutral AuCO, B3LYP gives an Au–C–O bond angle which is 7.7° too small compared to CCSD(T).

The dissociation energies of monogold-carbonyl compounds Au–CO^q ($q = -1, 0, +1$) decrease substantially from the positively to the negatively charged molecule (Table V). That is, Au⁺ binds carbon monoxide strongly (2.2 eV), whereas for AuCO⁻, we obtain an extremely weak Au–CO interaction of less than 0.1 eV at the coupled cluster level using LB set. This overall trend is correctly reproduced by

all methods including DFT. We mention that our PW91 results are in good agreement with previous results by Wu *et al.*⁶⁰ who obtained dissociation energies of 2.57 eV for AuCO⁺, 0.80 eV for AuCO, and 0.46 eV for AuCO⁻ using the same density functional. Our values for the dissociation energy of neutral AuCO are also in good agreement with Giordano *et al.*⁹¹ who obtained dissociation energies of 0.27 eV using CCSD(T) and 0.49 eV using the PW91 functional. Further, the calculated MP2 value for AuCO is substantially larger than the one given by Schwerdtfeger and Bowmaker,⁵⁶ as the basis sets used here are better suited for correlated calculations. In this paper, it was also noted that the Au–CO bond is stable only if relativistic effects are included.⁵⁶

If we consider the charge induced dipole (CID) interaction, $V_{\text{CID}}(r) = -q_{\text{Au}}^2 \alpha_{\text{CO}} / 2r^4$, where q_{Au} is the charge of the Au atom and α_{CO} is the polarizability of CO, we should expect some sizable CID interactions as the polarizability of CO is not that small (13.27 a.u. at the MP2 level of theory using the aug-cc-pVTZ basis set). However, the Au⁻–CO distance is rather large and repulsive forces start to dominate over the attractive CID interaction at bond distances below 3 Å. This results in a rather weak interaction with a dissociation energy strongly dependent on the method used. Note that the interaction between Au⁻ and Xe was also found to be extremely small.⁹² Using our SB set, the BSSE is very large for AuCO⁻ and leads to a negative binding energy at the (BSSE uncorrected) optimized distance. It is well-known that *ab initio* calculations yield large BSSEs for weak interactions in gold compounds⁹³ in contrast to DFT. For AuCO⁻, increasing the basis set, therefore, leads to rather long bond distances and very small dissociation energies. Our best estimate for AuCO⁻ is a dissociation energy of only about 0.1 eV. From the vibrational frequencies, we obtain a zero-point vibrational energy correction of 0.008 eV for the dis-

TABLE III. Spectroscopic properties of Au_2^q , $q=-1, 0, +1$. Distances r_e are in Å, dissociation energies D_e in eV (not corrected for the zero-point vibrational energy), and harmonic frequencies ω_e in cm^{-1} . SB set is used if not otherwise stated. Experimental values from Refs. 87, 88, and 90.

Method	r_e	D_e	ω_e
Au_2^+			
LSDA	2.569	2.879	164
BP86	2.645	2.338	144
PW91	2.644	2.385	145
PW91 ^a	2.603	2.499	148
B3LYP	2.687	2.032	132
B3LYP ^a	2.647	2.122	137
MP2	2.610	1.983	144
MP2 ^b	2.566	2.146	154
MP2 ^a	2.547	2.200	161
CCSD(T)	2.644	1.954	139
CCSD(T) ^b	2.613	2.047	139
CCSD(T) ^a	2.593	2.095	150
Expt.		2.32 ± 0.21	
Au_2			
LSDA	2.482	2.828	193
BP86	2.545	2.156	168
PW91	2.544	2.202	169
PW91 ^a	2.507	2.361	175
B3LYP	2.568	1.872	164
B3LYP ^a	2.535	2.007	168
MP2	2.460	2.309	197
MP2 ^b	2.432	2.582	205
MP2 ^a	2.422	2.680	211
CCSD(T)	2.509	2.088	180
CCSD(T) ^b	2.489	2.196	187
CCSD(T) ^a	2.477	2.272	187
Expt.	2.4715	2.29 ± 0.02	190.9
Au_2^-			
LSDA	2.585	2.419	150
BP86	2.670	1.874	131
PW91	2.667	1.922	132
PW91 ^a	2.626	1.996	134
B3LYP	2.709	1.583	121
B3LYP ^a	2.670	1.679	125
MP2	2.557	1.990	157
MP2 ^b	2.524	2.149	165
MP2 ^a	2.513	2.168	161
CCSD(T)	2.624	1.840	141
CCSD(T) ^b	2.605	1.894	143
CCSD(T) ^a	2.591	1.902	147
Expt.	2.582 ± 0.007	1.92 ± 0.15	149 ± 10

^aLB set.^bMB set.

sociation energy of AuCO^- which only slightly reduces the calculated CCSD(T) dissociation energy. The very weak bonding of CO to Au^- will make it difficult for future experiments to observe this molecule in the gas phase. Giordano *et al.* also report large BSSEs in their CCSD(T) calculations (about 80%) and a BSSE of 30% in their PW91 calculations, much larger compared to our calculations (see Table V), where LB set leads to negligible BSSEs for both density functionals PW91 and B3LYP. Furthermore, whereas in the DFT case, almost all of the BSSE comes from the gold

TABLE IV. Optimized geometries of AuCO^q , $q=1, 0, +1$. Distances are in Å and angles in degrees. SB set is used if not otherwise stated.

Method	r_{AuC}	r_{CO}	$\angle \text{AuCO}$
AuCO^+			
LSDA	1.861	1.122	180.0
BP86	1.910	1.130	180.0
PW91	1.907	1.128	180.0
PW91 ^a	1.893	1.127	180.0
B3LYP	1.956	1.116	180.0
B3LYP ^a	1.941	1.143	180.0
MP2	1.865	1.126	180.0
MP2 ^b	1.873	1.126	180.0
MP2 ^a	1.870	1.125	180.0
CCSD(T)	1.910	1.125	180.0
CCSD(T) ^b	1.924	1.120	180.0
CCSD(T) ^a	1.921	1.118	180.0
AuCO			
LSDA	1.935	1.146	142.4
BP86	1.999	1.155	141.2
PW91	1.993	1.154	141.0
PW91 ^a	1.974	1.153	141.5
B3LYP	2.060	1.139	140.1
B3LYP ^a	2.035	1.138	140.7
MP2	1.898	1.144	158.2
MP2 ^b	1.922	1.145	152.6
MP2 ^a	1.922	1.145	149.9
CCSD(T)	1.954	1.143	152.5
CCSD(T) ^b	1.989	1.138	150.8
CCSD(T) ^a	1.990	1.137	148.4
AuCO^-			
LSDA	2.088	1.174	119.2
BP86	2.225	1.180	117.9
PW91	2.212	1.178	118.0
PW91 ^a	2.188	1.177	118.4
B3LYP	2.502	1.153	114.5
B3LYP ^a	2.478	1.151	114.8
MP2	2.016	1.191	119.5
MP2 ^b	2.072	1.188	118.0
MP2 ^a	2.075	1.187	117.9
CCSD(T)	2.116	1.180	119.0
CCSD(T) ^b	2.314	1.162	115.3
CCSD(T) ^a	3.416	1.333	100.2

^aLB set.^bMB set.

basis set contributing to the total energy of the CO molecule; in the coupled cluster case, most of the BSSE comes from the CO basis set contributing to the total energy of Au^- . We also note that extending the basis sets from SB to LB leads to a shorter Au–C bond distance for PW91 but to a much larger bond distance for both MP2 and CCSD(T). This clearly demonstrates the different role of the basis set in Kohn-Sham calculations as compared to wave-function based theories. Nevertheless, none of the density functionals applied can describe the extremely weak Au^- –CO bond correctly. Moreover, the density functionals applied seem to overestimate the weak interaction between CO and Au^- and not underestimate it as one may naively expect.

The vibrational frequencies are given in Table VI. The B3LYP values for neutral AuCO are in good agreement with

TABLE V. Dissociation energies, BSSE errors Δ_{BSSE} , and BSSE corrected dissociation energies for AuCO^q , $q=+1, 0, -1$ (in eV). If not otherwise stated, SB set is used.

Method	AuCO^+			AuCO			AuCO^-		
	D_e	Δ_{BSSE}	$D_e - \Delta_{\text{BSSE}}$	D_e	Δ_{BSSE}	$D_e - \Delta_{\text{BSSE}}$	D_e	Δ_{BSSE}	$D_e - \Delta_{\text{BSSE}}$
LSDA	3.404	0.008	3.336	1.530	0.008	1.522	0.995	0.037	0.958
BP86	2.553	0.013	2.540	0.833	0.009	0.824	0.442	0.039	0.403
PW91	2.600	0.013	2.587	0.900	0.009	0.891	0.522	0.040	0.482
PW91 ^a	2.721	0.004	2.717	0.986	0.003	0.983	0.498	0.002	0.496
B3LYP	2.050	0.011	2.039	0.411	0.007	0.404	0.135	0.028	0.107
B3LYP ^a	2.151	0.003	2.148	0.472	0.002	0.470	0.113	0.002	0.111
MP2	2.637	0.278	2.359	1.032	0.395	0.637	0.756	0.582	0.174
MP2 ^b	2.560	0.186	2.374	0.802	0.192	0.610	0.460	0.245	0.215
MP2 ^a	2.601	0.135	2.466	0.800	0.130	0.671	0.374	0.119	0.255
CCSD(T)	2.314	0.348	1.966	0.818	0.446	0.372	0.460	0.541	-0.081
CCSD(T) ^b	2.208	0.168	2.040	0.549	0.169	0.380	0.150	0.137	0.013
CCSD(T) ^a	2.236	0.122	2.114	0.545	0.101	0.444	0.112	0.027	0.085

^aLB set.^bMB set.

the calculated values of Jiang and Xu^{94,95} who obtained 2066, 330, and 211 cm^{-1} for the CO stretching, Au–C stretching and AuCO bending mode respectively. Again the performance of the different density functionals varies widely. The AuCO^- results are more consistent with B3LYP having the largest C–O stretch vibrational frequency. Even for the positively charged AuCO^+ , the frequencies vary widely within the different DFT approximations. At the DFT level, we observe an increased redshift in the CO stretching frequency when moving from the positively charged to the neutral and the negatively charged gold atom or dimer as increased back bonding from Au into CO weakens the carbon oxygen bond considerably. However, we note the large change of the Au–C stretching and Au–C–O bending modes in AuCO^- when changing from SB to LB set, which again is indicative of a very weak Au–CO bond. Only B3LYP yields similar small frequencies as mixing in of exact exchange will diminish strong bonding due to overlap. We mention that our CCSD(T) result for the CO stretching frequency in AuCO changes from 2083 cm^{-1} to 2056 cm^{-1} due to anharmonicity

effects and is quite close to the experimental value of 2039 cm^{-1} obtained from matrix isolation infrared spectroscopy by Jiang and Xu.⁹⁴

The adiabatic ionization potentials and electron affinities of AuCO are given in Table II. The DFT results are similar to each other with the notable exception of the LSDA functional. Experimental values are not available but our best coupled cluster results agree quite well with the B3LYP values. We note that the MP2 value for the electron affinity of AuCO is far too low. CO bonding to Au leads to a substantial decrease in both the ionization potential and electron affinity.

The optimized geometries of Au_2CO^q with $q=-1, 0, +1$ are given in Table VII. Here, we studied two possible minimum geometries, the end-on structure ($C_{\infty v}$ or C_s symmetry) with CO attached to one Au atom in a *trans* fashion and the side-on structure with CO bridging symmetrically two Au atoms (C_{2v} symmetry) (see Fig. 1). In all cases, the end-on structure represents the global minimum, which is a linear structure except for the negatively charged system. In agreement with Socaciu *et al.*,³⁰ we obtain a linear Au–Au–C

TABLE VI. Harmonic vibrational frequencies (in cm^{-1}) for AuCO^q , $q=+1, 0, -1$. The experimental CO stretching mode for AuCO is 2039.3 cm^{-1} from Ref. 94. The experimentally derived harmonic frequency for free CO is 2169.8 cm^{-1} (Ref. 90). Basis set SB used if not otherwise stated.

	Sym	LSDA	BP86	PW91	PW91 ^a	B3LYP	B3LYP ^a	MP2	MP2 ^b	MP2 ^a	CCSD(T)	CCSD(T) ^a
CO	Σ	2182	2117	2129	2133	2207	2212	2137	2137	2138	2145	2175
AuCO^+	Π	332	314	314	315	308	311	356	354	349	370	323
	Σ	479	425	427	436	378	390	456	450	453	416	407
	Σ	2268	2202	2212	2211	2304	2303	2218	2215	2215	2249	2283
AuCO	A'	263	248	250	258	227	234	147	192	209	218	201
	A'	490	423	428	450	354	372	444	429	438	407	374
	A'	2037	1972	1981	1979	2068	2067	2053	2026	2015	2056	2083
AuCO^-	A'	245	193	199	202	76	84	283	251	248	230	44
	A'	433	371	375	377	297	299	475	420	422	411	125
	A'	1835	1796	1804	1803	1962	1963	1742	1754	1755	1782	2140

^aLB set.^bMB set.

TABLE VII. Optimized geometries of digold carbon monoxide clusters. Distances given in Å and angles in degrees. All side-on structure are of C_{2v} symmetry, and all end-on structures are either $C_{\infty v}$ or C_s . SB set is used if not otherwise stated.

Method	Symmetry	$r(\text{AuAu})$	$r(\text{AuC})$	$r(\text{AuO})$	$\angle \text{AuAuC}$	$\angle \text{AuCO}$
Au_2CO^+						
LSDA	$C_{\infty v}$	2.545	1.878	1.125	180.0	180.0
	C_{2v}	2.833	1.948	1.154	43.4	133.4
BP86	$C_{\infty v}$	2.640	1.927	1.133	180.0	180.0
	C_{2v}	3.023	1.999	1.164	40.9	130.9
PW91	$C_{\infty v}$	2.640	1.923	1.131	180.0	180.0
	C_{2v}	3.015	1.996	1.163	40.9	130.9
PW91 ^a	$C_{\infty v}$	2.588	1.911	1.131	180.0	180.0
	C_{2v}	1.943	1.981	1.162	42.0	132.0
B3LYP	$C_{\infty v}$	2.678	1.968	1.119	180.0	180.0
	C_{2v}	3.189	2.037	1.150	38.5	128.5
B3LYP ^a	$C_{\infty v}$	2.634	1.953	1.117	180.0	180.0
	C_{2v}	3.108	2.018	1.149	39.6	129.6
MP2	$C_{\infty v}$	2.591	1.866	1.129	180.0	180.0
	C_{2v}	2.792	1.914	1.148	43.2	133.2
MP2 ^b	$C_{\infty v}$	2.533	1.877	1.129	180.0	180.0
	C_{2v}	2.745	1.925	1.146	44.5	134.5
CCSD(T)	$C_{\infty v}$	2.643	1.914	1.127	180.0	180.0
	C_{2v}	2.929	1.963	1.154	41.8	131.8
Au_2CO						
LSDA	$C_{\infty v}$	2.469	1.875	1.137	180.0	180.0
	C_{2v}	3.147	1.947	1.172	36.1	126.1
BP86	$C_{\infty v}$	2.525	1.922	1.145	180.0	180.0
	C_{2v}	3.300	2.005	1.182	34.6	124.6
PW91	$C_{\infty v}$	2.524	1.918	1.144	180.0	180.0
	C_{2v}	3.292	2.000	1.180	34.6	124.6
PW91 ^a	$C_{\infty v}$	2.492	1.906	1.143	180.0	180.0
	C_{2v}	3.249	1.984	1.180	35.1	125.1
B3LYP	$C_{\infty v}$	2.549	1.957	1.129	180.0	180.0
	C_{2v}	3.384	2.035	1.168	33.7	123.7
B3LYP ^a	$C_{\infty v}$	2.520	1.944	1.128	180.0	180.0
	C_{2v}	3.341	2.017	1.168	34.1	124.1
MP2	$C_{\infty v}$	2.465	1.849	1.140	180.0	180.0
	C_{2v}	3.072	1.907	1.172	36.6	126.6
MP2 ^b	$C_{\infty v}$	2.429	1.860	1.139	180.0	180.0
	C_{2v}	3.053	1.919	1.169	37.3	127.3
CCSD(T)	$C_{\infty v}$	2.517	1.896	1.138	180.0	180.0
	C_{2v}	3.196	1.953	1.176	35.1	125.1
Au_2CO^-						
LSDA	C_s	2.564	1.959	1.175	179.1	137.1
	C_{2v}	3.266	2.017	1.181	35.9	125.9
BP86	C_s	2.644	2.031	1.185	179.9	133.9
	C_{2v}	3.147	1.947	1.172	36.1	126.1
PW91	C_s	2.641	2.023	1.183	179.9	134.1
	C_{2v}	3.478	2.086	1.188	33.5	123.5
PW91 ^a	C_s	2.601	2.004	1.182	179.8	135.3

TABLE VII. (Continued.)

Method	Symmetry	$r(\text{AuAu})$	$r(\text{AuC})$	$r(\text{AuO})$	$\angle \text{AuAuC}$	$\angle \text{AuCO}$
	C_{2v}	3.424	2.067	1.187	34.1	124.1
B3LYP	C_s	2.676	2.079	1.171	179.1	131.5
	C_{2v}	3.617	2.143	1.172	32.5	122.5
B3LYP ^a	C_s	2.640	2.058	1.170	179.0	132.7
	C_{2v}	3.567	2.122	1.171	32.8	122.8
MP2	C_s	2.549	1.907	1.182	170.7	142.6
	C_{2v}	3.211	1.924	1.191	33.5	123.5
MP2 ^b	C_s	2.506	1.918	1.176	170.8	143.6
	C_{2v}	3.179	1.976	1.178	36.5	126.5
CCSD(T)	C_s	2.626	1.977	1.185	177.5	135.5
	C_{2v}	3.298	1.973	1.186	33.3	123.3

^aLB set.^bMB set.

angle for the neutral compound. Calculations of the $\text{Au}_2\text{-CO}$ bending potential curve reveal that the metastable state of C_{2v} symmetry is reached through a path which involves near dissociation of CO from Au_2 . The difference between the *ab initio* and DFT bonding parameters can be significant, especially for the negatively charged system, but the situation here is not as dramatic as in the case of AuCO^- .

We note again the very large BSSE for the wavefunction based methods in contrast to DFT (Table VIII). Here, we could not optimize the molecules at the coupled cluster level with either the MB or the LB set as the calculations become prohibitively expensive. Nevertheless, the BSSE corrected results clearly indicate that Au_2CO^- is reasonably stable in contrast to AuCO^- with a dissociation energy of 0.34 eV, in very good agreement with the B3LYP result of 0.40 eV. Except for the B3LYP functional, all the other applied DFT methods seem to overbind. However, for Au_2CO^- , our dissociation energy is considerably lower than the one estimated by Lütgens using photoelectron spectroscopy,⁹⁶ who obtained 0.9 eV for the desorption

threshold. Even though our BSSE is still too large to obtain accurate dissociation energies, we believe that the experimental value is probably too high. In contrast, our pure generalized gradient approximation functionals are much closer to this experimental value. Nevertheless, we note that the dissociation energy decreases from the positively to the negatively charged species as this is the case for AuCO^q with $q=-1, 0, +1$, and this trend is reproduced by all applied methods.

For the Au_2CO^q series with $q=-1, 0, +1$, we obtain a similar pattern compared to AuCO^q ; i.e., for the positively charged species, the CO stretching frequency increases upon adsorption, slightly decreases for the neutral molecule, and substantially decreases for the negatively charged species (except for the weakly bound AuCO^- at the coupled cluster level of theory) (Table IX). The effect of the charge on $\nu(\text{CO})$ has been studied for other metals as well, and it is well-known that the charge has a significant influence on the CO stretching frequency, with larger clusters tend to have a smaller effect as the charge smears out over the metal cluster.⁹⁷ It can also be seen that the Au-Au stretch frequency is only slightly affected by the adsorption of CO.

It is difficult to estimate accurate values for the ionization potential and electron affinity of Au_2CO as we could not perform coupled cluster calculations with the larger basis set. If we take the difference between Au_2 and Au_2CO and add this to our most accurate CCSD(T) values using the LB set for Au_2 , we estimate an ionization potential of 9.0 eV and electron affinity of about 1.1 eV for Au_2CO . This is close to the calculated B3LYP value. We note the large variation in the electron affinity with the different density functionals applied. As in the case for AuCO , CO bonding to Au_2 leads to a substantial decrease in both the ionization potential and electron affinity.

Finally, the dipole moments for the neutral molecules are listed in Table X. We note that for AuCO and Au_2CO , there is appreciable charge transfer from Au into CO; i.e., for the neutral compounds, we have the Mulliken charges $\text{Au}^{0.23}\text{-C}^{-0.10}\text{-O}^{-0.13}$ and $\text{Au}^{-0.78}\text{-Au}^{1.16}\text{-C}^{-0.05}\text{-O}^{-0.33}$ at

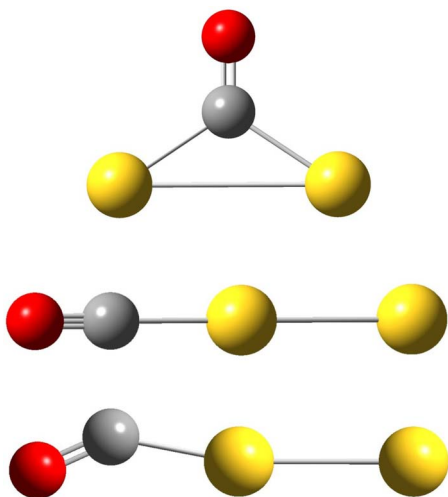


FIG. 1. (Color online) From top to bottom: MP2 structures for Au_2CO (C_{2v}), Au_2CO (C_{2v}), and Au_2CO^- (C_s).

TABLE VIII. Dissociation energies, BSSE errors Δ_{BSSE} , and BSSE corrected dissociation energies for Au_2CO^q , $q = +1, 0, -1$ (in eV). The correct symmetry group for the side-on and end-on structures are given in Table VII. SB set is used if not otherwise stated.

Method	Struct.	Au_2CO^+			Au_2CO			Au_2CO^-		
		D_e	Δ_{BSSE}	$D_e - \Delta_{\text{BSSE}}$	D_e	Δ_{BSSE}	$D_e - \Delta_{\text{BSSE}}$	D_e	Δ_{BSSE}	$D_e - \Delta_{\text{BSSE}}$
LSDA	End on	2.847	0.040	2.807	2.452	0.037	2.415	1.607	0.034	1.573
	Side on	2.667	0.041	2.626	1.391	0.027	1.364	1.304	0.036	1.268
BP86	End on	2.038	0.034	2.004	1.628	0.032	1.596	0.904	0.038	0.866
	Side on	1.604	0.031	1.573	0.486	0.022	0.464	0.502	0.032	0.470
PW91	End on	2.091	0.029	2.062	1.696	0.031	1.665	0.996	0.031	0.865
	Side on	1.701	0.029	1.672	0.589	0.023	0.566	0.609	0.033	0.576
PW91 ^a	End on	2.190	0.032	2.158	1.778	0.029	1.749	1.033	0.021	1.012
	Side on	1.777	0.047	1.730	0.614	0.042	0.572	0.611	0.037	0.574
B3LYP	End on	1.662	0.026	1.636	1.192	0.027	1.165	0.523	0.025	0.498
	Side on	0.938	0.021	0.917	-0.156	0.018	-0.174	-0.006	0.026	-0.032
B3LYP ^a	End on	1.753	0.030	1.723	1.266	0.025	1.241	0.556	0.160	0.396
	Side on	1.008	0.006	1.002	-0.129	0.036	-0.165	0.001	0.031	-0.030
MP2	End on	2.529	0.463	2.066	2.244	0.546	1.698	1.079	0.552	0.527
	Side on	1.956	0.888	1.068	1.161	1.057	0.104	0.727	1.091	-0.364
MP2 ^b	End on	2.435	0.229	2.205	2.061	0.256	1.805	0.868	0.247	0.620
	Side on	1.545	0.353	1.191	0.513	0.405	0.108	0.031	0.414	-0.385
CCSD(T)	End on	2.161	0.832	1.273	1.790	0.974	0.816	0.864	0.527	0.337
	Side on	1.695	0.907	0.788	0.694	1.053	-0.359	1.375	1.205	0.170

^aLB set.^bMB set.

the B3LYP level of theory. This explains the large dipole moments obtained. For AuCO^- and Au_2CO^- , we get a slightly increased charge transfer compared to the neutral molecules, i.e., $\text{Au}^{-0.75}-\text{C}^{-0.06}-\text{O}^{-0.19}$ and

$\text{Au}^{0.69}-\text{Au}^{-1.16}-\text{C}^{-0.06}-\text{O}^{-0.46}$. Hence, there is considerable Coulomb repulsion between CO and Au or Au_2 in the negatively charged species, which may rationalize the low stabilities of these systems. The highest occupied molecular orbit-

TABLE IX. Harmonic vibrational frequencies of Au_2CO^q ($q = +1, 0, -1$). The vibrational frequencies are given in cm^{-1} . The experimental CO stretching mode for Au_2CO is 2131.9 cm^{-1} from Ref. 94. SB set is used if not otherwise stated.

		LSDA	BP86	PW91	PW91 ^a	B3LYP	B3LYP ^a	MP2	MP2 ^b
CO	Σ	2182	2117	2129	2133	2207	2212	2137	2137
Au_2^+CO	Π	33	35	35	35	40	42	52	55
	Σ	149	129	129	134	123	129	139	152
	Π	355	334	333	336	329	333	406	395
	Σ	475	414	417	430	372	384	472	463
	Σ	2241	2175	2185	2182	2276	2275	2203	2202
Au_2CO	Π	50	45	45	46	45	46	60	64
	Σ	194	176	176	180	169	172	193	203
	Π	378	347	347	355	333	342	437	428
	Σ	479	425	428	438	382	391	500	489
	Σ	2154	2086	2096	2092	2185	2182	2128	2122
Au_2^-CO	A'	49	46	46	48	45	47	42	62
	A''	77	73	74	76	69	72	50	54
	A'	154	133	134	138	126	129	162	157
	A'	297	276	278	284	262	269	324	338
	A'	489	426	432	436	385	392	465	482
	A'	1850	1778	1788	1788	1837	1835	1769	1728

^aLB set.^bMB set.

TABLE X. Dipole moments for the neutral species AuCO and Au₂CO (in D). SB set is used if not otherwise stated.

	LSDA	BP86	PW91	PW91 ^a	B3LYP	B3LYP ^a	MP2	MP2 ^b	MP2 ^a
CO	0.222	0.182	0.187	0.193	0.095	0.103	0.297	0.297	0.287
AuCO	0.410	0.387	0.407	0.415	0.441	0.468	1.805	1.627	1.591
Au ₂ CO C _s /C _{∞v}	1.365	1.661	1.588	1.483	2.069	1.964	1.435	1.243	...
Au ₂ CO C _{2v}	1.944	1.833	1.893	1.862	2.010	1.989	3.757	3.832	...

^aLB set.^bMB set.

als in AuCO⁻ and Au₂CO⁻ consist mainly of an antibonding orbital between the CO unit and gold, with most of the density located at the gold unit consisting of an admixture between Au 6s and 5d. In fact, for AuCO⁻, the highest occupied molecular orbital becomes very diffuse upon CO binding resulting in a positive orbital energy (even for the local density functional calculations) using the small basis set without the additional diffuse s functions for gold.

IV. CONCLUSION

The properties of Au_nCO^q compounds with n=1, 2 and q=-1, 0, +1 have been investigated with both density functional and wave-function based methods using our newly developed correlation-consistent basis set for gold. A serious problem in these calculations is the large basis-set superposition error in wave-function based calculations. The BSSE can be greatly reduced by decontracting the f functions of the basis set and introducing additional high angular momentum functions. Unfortunately, this leads to a high computational demand and calculations beyond the triatomic compound AuCO becomes unfeasible. The performance of the various density functionals applied varies widely with perhaps the B3LYP functional which includes exact exchange performing reasonably well. The situation will probably improve for larger negatively charged gold clusters as the charge will be smeared out of the whole system. Nevertheless, the application of DFT to CO adsorption on larger gold clusters or surfaces, therefore, remains somewhat questionable.

ACKNOWLEDGMENTS

We are grateful to the Alexander von Humboldt Foundation for support. This work was financed by a Marsden grant through the Royal Society of New Zealand.

¹G. C. Bond, C. Louis, and D. T. Thompson, *Catalysis by Gold*, Catalytic Science Series Vol. 6 (Imperial College Press, London, 2006).

²M. Haruta, *Catal. Today* **36**, 153 (1997).

³G. C. Bond, *Catal. Today* **72**, 5 (2002).

⁴M. Haruta, *Chem. Rec.* **3**, 75 (2003).

⁵D. T. Thompson, *Appl. Catal., A* **243**, 201 (2003).

⁶T. Ishida and M. Haruta, *Angew. Chem., Int. Ed.* **46**, 7154 (2007).

⁷M. B. Cortie, *Gold Bull.* **37/1**, 12 (2004).

⁸D. S. Cameron, *Gold Bull.* **36**, 17 (2003).

⁹J. Hagen, L. D. Socaciu, U. Heiz, T. M. Bernhardt, and L. Wöste, *Eur. Phys. J. D* **24**, 1434 (2003).

¹⁰Q. Sun, Q. Wang, B. K. Rao, and P. Jena, *Phys. Rev. Lett.* **93**, 186803 (2004).

¹¹R. C. Elder, K. Ludwig, J. N. Cooper, and M. K. Eidsness, *J. Am. Chem. Soc.* **107**, 5024 (1985).

¹²H. Gu, P. L. Ho, E. Tong, L. Wang, and B. Xu, *Nano Lett.* **3**, 1261

(2003).

¹³L. Levchenko, A. Sadkov, N. Lariontseva, E. Koldasheva, A. Shilova, and A. Shilov, *J. Inorg. Biochem.* **88**, 251 (2002).

¹⁴T. Niazov, V. Pavlov, Y. Xiao, R. Gil, and I. Willner, *Nano Lett.* **4**, 1683 (2004).

¹⁵L. Fu, N. Q. Wu, H. Yang, F. Qu, D. L. Johnson, M. C. Kung, H. H. Kung, and V. P. Dravid, *J. Phys. Chem. B* **109**, 3704 (2005).

¹⁶J.-H. Liu, A.-Q. Wang, Y.-S. Chi, H.-P. Lin, and C.-Y. Mou, *J. Phys. Chem. B* **109**, 40 (2005).

¹⁷A. M. Venezia, G. Pantaleo, A. Longo, G. D. Carlo, M. P. Casaletto, F. L. Liotta, and G. Deganello, *J. Phys. Chem. B* **109**, 2821 (2005).

¹⁸S. Arrii, F. Morfin, A. J. Renouprez, and J. L. Rousset, *J. Am. Chem. Soc.* **126**, 1199 (2004).

¹⁹M. Comotti, C. Della Pina, R. Matarrese, and M. Rossi, *Angew. Chem., Int. Ed.* **43**, 5812 (2004).

²⁰I. Balteanu, O. Petru Balaj, B. S. Fox, M. K. Beyer, Z. Bastl, and V. E. Bondybey, *Phys. Chem. Chem. Phys.* **5**, 1213 (2003).

²¹G. J. Hutchings, *Gold Bull.* **37**, 1 (2004).

²²Q. Fu, H. Saltsburg, and M. Flytzani-Stephanopoulos, *Science* **301**, 935 (2003).

²³C. W. Corti, R. J. Holliday, and D. T. Thompson, *Gold Bull.* **35**, 111 (2002).

²⁴M. Valden, X. Lai, and D. W. Goodman, *Science* **281**, 1647 (1998).

²⁵S. Schimpf, M. Lucas, C. Mohr, U. Rodemerck, A. Brückner, J. Radnik, H. Hofmeister, and P. Claus, *Catal. Today* **72**, 63 (2002).

²⁶P. Pyykkö, *Angew. Chem.* **116**, 4512 (2004).

²⁷S. Gilb, P. Weis, F. Furche, R. Ahlrichs, and M. M. Kappes, *J. Chem. Phys.* **116**, 4094 (2002).

²⁸F. Furche, R. Ahlrichs, P. Weis, C. Jacob, S. Gilb, T. Bierweiler, and M. M. Kappes, *J. Chem. Phys.* **117**, 6982 (2002).

²⁹P. Schwerdtfeger, *Angew. Chem., Int. Ed.* **42**, 1892 (2003).

³⁰L. D. Socaciu, J. Hagen, T. M. Bernhardt, L. Wöste, U. Heiz, H. Häkkinen, and U. Landman, *J. Am. Chem. Soc.* **125**, 10437 (2003).

³¹B. Yoon, H. Häkkinen, U. Landman, A. S. Wörz, J.-M. Antonietti, S. Abbet, K. Judai, and U. Heiz, *Science* **307**, 403 (2005).

³²N. Lopez and J. K. Nørskov, *J. Am. Chem. Soc.* **124**, 11262 (2002).

³³H. Häkkinen and U. Landman, *J. Am. Chem. Soc.* **123**, 9704 (2001).

³⁴A. Sanchez, S. Abbet, U. Heiz, W.-D. Schneider, H. Häkkinen, R. N. Barnett, and U. Landmann, *J. Phys. Chem. A* **103**, 9573 (1999).

³⁵G. Bilalbegović, *Vacuum* **71**, 165 (2003).

³⁶M. Lahav, T. Sehayek, A. Vaskevich, and I. Rubinstein, *Angew. Chem., Int. Ed.* **42**, 5576 (2003).

³⁷J. Li, X. Li, H.-J. Zhai, and L.-S. Wang, *Science* **299**, 864 (2003).

³⁸J. Wang, G. Wang, and J. Zhao, *Chem. Phys. Lett.* **380**, 716 (2003).

³⁹J. Wang, G. Wang, and J. Zhao, *Phys. Rev. B* **66**, 035418 (2002).

⁴⁰A. Pinto, A. R. Pennisi, and G. Faraci, *Phys. Rev. B* **51**, 5315 (1995).

⁴¹P. Pyykkö and N. Runeberg, *Angew. Chem., Int. Ed.* **41**, 2174 (2002).

⁴²L.-P. Jiang, S. Xu, J.-M. Zhu, J.-R. Zhang, J.-J. Zhu, and H.-Y. Chen, *Inorg. Chem.* **43**, 5877 (2004).

⁴³J. Aizpurua, P. Hanarp, D. S. Sutherland, M. Käll, G. W. Bryant, and F. J. G. de Abajo, *Phys. Rev. Lett.* **90**, 057401 (2003).

⁴⁴Z. Ning, J. Chen, S. Hou, J. Zhang, Z. Liang, J. Zhang, and R. Han, *Phys. Rev. B* **72**, 155403 (2005).

⁴⁵T. Ono and K. Hirose, *Phys. Rev. Lett.* **94**, 206806 (2005).

⁴⁶S. Stojkovic, C. Joachim, L. Grill, and F. Moresco, *Chem. Phys. Lett.* **408**, 134 (2005).

⁴⁷E. Z. da Silva, A. J. R. da Silva, and A. Fazzio, *Comput. Mater. Sci.* **30**, 73 (2004).

⁴⁸H.-J. Zhai, B. Kiran, and L.-S. Wang, *J. Chem. Phys.* **121**, 8231 (2004).

⁴⁹E. Tosatti, S. Prestipino, S. Kostlmeier, A. Dal Corso, and F. D. Di Tolla, *Science* **291**, 288 (2001).

⁵⁰D. Sánchez-Portal, E. Artacho, J. Junquera, P. Ordejón, A. García, and J.

- M. Soler, *Phys. Rev. Lett.* **83**, 3884 (1999).
- ⁵¹ J. A. Torres, E. Tosatti, A. Dal Corso, F. E. J. J. Kohanoff, F. D. Di Tolla, and J. M. Soler, *Surf. Sci. Lett.* **426**, L441 (1999).
- ⁵² J. Pascual, J. Mendex, J. Gomez-Herrero, A. M. Baro, N. Garcia, U. Landman, W. Luedtke, E. Bogachek, and H.-P. Cheng, *Science* **267**, 1793 (1995).
- ⁵³ J.-S. Lin, S.-P. Ju, and W.-J. Lee, *Phys. Rev. B* **72**, 085448 (2005).
- ⁵⁴ Y. Kondo and K. Takayanagi, *Science* **289**, 606 (2000).
- ⁵⁵ H. Huber, D. McIntosh, and G. A. Ozin, *Inorg. Chem.* **16**, 975 (1977).
- ⁵⁶ P. Schwerdtfeger and G. A. Bowmaker, *J. Chem. Phys.* **100**, 4487 (1994).
- ⁵⁷ X. Ding, Z. Li, J. Yang, J. G. Hou, and Q. Zhu, *J. Chem. Phys.* **120**, 9594 (2004); **121**, 2558 (2004).
- ⁵⁸ H.-J. Zhai and L.-S. Wang, *J. Chem. Phys.* **122**, 051101 (2005).
- ⁵⁹ Y. Wang and X. G. Gong, *J. Chem. Phys.* **125**, 124703 (2006).
- ⁶⁰ X. Wu, L. Senapati, S. K. Nayak, A. Selloni, and M. Hajaligol, *J. Chem. Phys.* **117**, 4010 (2002).
- ⁶¹ B. Liang and L. Andrews, *J. Phys. Chem. A* **104**, 9156 (2000).
- ⁶² J. D. Stiehl, T. S. Kim, S. M. McClure, and C. B. Mullins, *J. Am. Chem. Soc.* **126**, 1606 (2004).
- ⁶³ T. M. Wallis, N. Nilius, and W. Ho, *J. Chem. Phys.* **119**, 2296 (2003).
- ⁶⁴ S. A. Varganov, R. M. Olson, M. S. Gordon, and H. Metiu, *J. Chem. Phys.* **119**, 2531 (2003).
- ⁶⁵ G. Mills, M. S. Gordon, and H. Metiu, *Chem. Phys. Lett.* **359**, 493 (2002).
- ⁶⁶ B. E. Salisbury, W. T. Wallace, and R. L. Whetten, *Chem. Phys.* **262**, 131 (2000).
- ⁶⁷ S. Carrettin, Y. Hao, V. Aguilar-Guerrero, B. C. Gates, S. Trasobares, J. J. Calvino, and A. Corma, *Chem.-Eur. J.* **13**, 7771 (2007).
- ⁶⁸ A. Ueda and M. Haruta, *Gold Bull.* **32**, 3 (1999).
- ⁶⁹ H. Sakurai and M. Haruta, *Catal. Today* **29**, 361 (1996).
- ⁷⁰ H. Sakurai, A. Ueda, T. Kobayashi, and M. Haruta, *Chem. Commun. (Cambridge)* **1997**, 271.
- ⁷¹ D. Andreeva, *Gold Bull.* **35**, 82 (2002).
- ⁷² Q.-M. Hu, K. Reuter, and M. Scheffler, *Phys. Rev. Lett.* **98**, 176103 (2007).
- ⁷³ P. Pyykkö, *Chem. Rev. (Washington, D.C.)* **88**, 563 (1988).
- ⁷⁴ T. Söhnel, H. Hermann, and P. Schwerdtfeger, *Angew. Chem., Int. Ed.* **40**, 4381 (2001).
- ⁷⁵ P. Schwerdtfeger, *Heteroat. Chem.* **13**, 578 (2002).
- ⁷⁶ S. H. Vosko, L. Wilk, and M. Nusair, *Can. J. Phys.* **58**, 1200 (1980).
- ⁷⁷ J. P. Perdew and Y. Wang, *Phys. Rev. B* **45**, 13244 (1992).
- ⁷⁸ J. P. Perdew, J. A. Chevary, S. H. Vosko, K. A. Jackson, M. R. Pederson, D. J. Singh, and C. Foilhais, *Phys. Rev. B* **46**, 6671 (1992).
- ⁷⁹ C. Lee, W. Yang, and R. G. Parr, *Phys. Rev. B* **37**, 785 (1988).
- ⁸⁰ A. D. Becke, *J. Chem. Phys.* **98**, 1372 (1993).
- ⁸¹ M. J. Frisch, G. W. Trucks, H. B. Schlegel *et al.*, GAUSSIAN 03, revision C.02, Gaussian, Inc., Pittsburgh, PA, 2003.
- ⁸² T. H. Dunning, Jr., *J. Chem. Phys.* **90**, 1007 (1989).
- ⁸³ D. Andrae, U. Häußermann, M. Dolg, H. Stoll, and H. Preuss, *Theor. Chem. Acc.* **77**, 123 (1990).
- ⁸⁴ S. F. Boys and F. Bernardi, *Mol. Phys.* **19**, 553 (1970).
- ⁸⁵ E. Eliav, U. Kaldor, and Y. Ishikawa, *Phys. Rev. A* **49**, 1724 (1994).
- ⁸⁶ M. A. Cheeseman and J. R. Eyler, *J. Phys. Chem.* **96**, 1982 (1992).
- ⁸⁷ J. Ho, K. M. Ervin, and W. C. Lineberger, *J. Chem. Phys.* **93**, 6987 (1990).
- ⁸⁸ G. A. Bishea and M. D. Morse, *J. Chem. Phys.* **95**, 5646 (1991).
- ⁸⁹ C. E. Moore, *Atomic Energy Levels*, Natl. Bur. Stand. (U. S.), Circ. No. 467 (U.S. GPO, Washington, DC, 1958).
- ⁹⁰ K. P. Huber and G. Herzberg, *Constants of Diatomic Molecules*, Molecular Spectra and Molecular Structure, Vol. 4 (Van Nostrand, New York, 1979).
- ⁹¹ L. Giordano, J. Carrasco, C. D. Valentin, F. Illas, and G. Pacchioni, *J. Chem. Phys.* **124**, 174709 (2006).
- ⁹² P. Pyykkö, *J. Am. Chem. Soc.* **117**, 2067 (1995).
- ⁹³ J. R. Rakow, "Quantenchemische Berechnung der Adsorption von organischen Molekülen auf Goldoberflächen," Master's thesis, Universität Münster, 2004.
- ⁹⁴ L. Jiang and Q. Xu, *J. Phys. Chem. A* **109**, 1026 (2005).
- ⁹⁵ Q. Xu and L. Jiang, *J. Phys. Chem. A* **110**, 2655 (2006).
- ⁹⁶ G. Lütgens, Ber. Forschungszent. Juelich [JUEL-3940, Zentralbibliothek (ZB)-Verlag], p. 1; <http://hdl.handle.net/2128/172>
- ⁹⁷ A. Fielicke, G. von Helden, G. Meijer, D. B. Pedersen, B. Simard, and D. M. Rayner, *J. Chem. Phys.* **124**, 194305 (2006).